

Neurons May Live for Decades with Neurofibrillary Tangles

RENEE MORSCH BS, WILLIAM SIMON PHD, AND PAUL D. COLEMAN PHD

Abstract. Neurons containing neurofibrillary tangles (NFT) are one of the pathological hallmarks of Alzheimer disease (AD). It is known that this population of neurons express gene products and thus function to some degree, but it is unknown how long these neurons may survive with NFT. It is also thought that the formation of NFT results in the death of neurons. Using quantitative data on neuron loss and NFT formation as a function of disease duration, we have generated a computer program that models both the degeneration of CA1 hippocampal neurons and the formation of NFT in these neurons in AD. Modeling various neuron survival times with NFT and altering selected assumptions upon which the models are based, we arrive at the conclusions that 1) CA1 hippocampal neurons survive with NFT for about 20 years, and 2) NFT may not be obligatory for death of CA1 hippocampal neurons in AD.

Key Words: Alzheimer disease; Neuron death; Neurofibrillary tangles.

INTRODUCTION

Alzheimer disease (AD) is characterized clinically by severe memory defects, cognitive decline, personality changes, and functional limitations. Neuropathologically, this disease is recognized by its hallmark features: senile plaques (SP) and neurofibrillary tangles (NFT) (1), as well as regionally specific neuronal loss (2). Recent evidence has shown that AD pathology may exist in aged persons without clinically detectable dementia (3, 4, 5). Additionally, the Braaks (6) have identified NFT, as well as SP, in the brains of people aged 26–30 yr. Although this is rare, with advancing age it becomes more and more probable that these pathologic changes will be present, particularly in the entorhinal cortex and hippocampal formation. In fact, in the oldest old, less than 1% of the brains surveyed displayed no neurofibrillary change (6). Clearly NFT are among the early, preclinical, abnormalities in AD.

NFT bearing neurons continue to express RNA (7, 8), but at levels that are reduced when compared with NFT-free neurons in both AD and control brain. It is also known that neurons containing NFT express selected gene products and that this population can be seen in abundance (9, 10). Thus it is apparent that neurons continue to survive and express a variety of gene products for some currently undefined period of time after NFT appear in their cytoplasm. We present here new quantitative data on the percentage of CA1 neurons bearing NFT, which combined with recent quantitative data on numbers of neurons and of neurons containing NFT in

hippocampal zones of AD and control cases as a function of age (2, 11, 12) and disease duration (11), allow the construction of models which provide estimates of how long, on average, a CA1 neuron can survive with a neurofibrillary tangle. These models also make it possible to estimate the proportion of CA1 neurons that die via an NFT-dependent pathway.

In this study we derive 4 models based on existing data regarding the loss of neurons (11, 12) and the formation of NFT (11, new data presented here) in CA1 of AD hippocampus, both as a function of disease duration. These models estimate that CA1 neurons containing NFT survive for approximately 20 yr. Model IV, which best fits the data, also indicates that it is not necessary to assume that NFT are directly related to the death of CA1 neurons in AD.

MATERIALS AND METHODS

West, using 38 controls (12), and Bobinski, using 16 AD and 5 controls (11), estimated the total number of CA1 neurons in normal aging and AD using unbiased stereological techniques. Bobinski (11) also used these methods to estimate the total number of tangles in CA1 in their 21 cases. The West data were expressed as a function of age, while the Bobinski data were expressed as a function of both age and of disease duration (since first report of symptoms). To determine the percentage of live neurons bearing NFT in CA1, we sampled 17 AD and 3 control brains (see Table 1 for characteristics). Stereological methodology was not used to obtain these data. The 20 cases newly presented here were embedded in paraffin and cut at 7 μ m. The sections were stained using a modified Bielschowsky stain (13). CA1 pyramidal neurons were counted at 200 \times magnification, starting at the CA2-CA1 boundary and advancing systematically to every other field. Five fields per case were counted and data from these 5 fields were averaged. Both the total number of neurons and the number of tangle bearing neurons in each field were counted to obtain the percentage of neurons bearing NFT. Ghost tangles were not counted. Figure 1 illustrates the classification of neurons.

A series of 4 models was developed based on all 3 available data sets (West, Bobinski, new data presented here) to estimate

From the Alzheimer Disease Center and the Departments of Neurobiology and Anatomy (RM, PDC) and Biochemistry and Biophysics (WS), University of Rochester Medical Center, Rochester, New York.

Correspondence to: Paul D. Coleman, PhD, Alzheimer Disease Center, University of Rochester Medical Center, 601 Elmwood Avenue, Box 603, Rochester, NY 14642.

This work was supported by grants from the NIA (LEAD AG09016, ROI AG14441, and the Rochester Alzheimer Disease Center AG08665), the American Health Assistance Foundation and the Markey Fund.

TABLE 1
Clinical Characteristics of Cases Newly Presented Here

	Case #	Age	CDR ¹	Duration of AD
AD	1	74	n/a	4
	2	89	5	6
	3	69	5	8
	4	62	5	8
	5	78	5	8
	6	81	2	8
	7	84	4	10
	8	90	5	11
	9	67	4	12
	10	91	5	12
	11	83	5	14
	12	93	5	14
	13	79	5	15
	14	84	5	15
	15	86	5	15
	16	90	5	23
	17	90	5	25
Control	18	n/a	0	—
	19	66	0	—
	20	91	0	—

¹ CDR refers to clinical dementia rating, and is measured on a scale of 0 (nondemented) to 5 (most severe dementia).

the average length of time a neuron remains alive after it has formed NFT. The initial model was based on (1) the rate of neuron loss in CA1 after the onset of symptoms, estimated as 500,000 cells per yr (2, 11, 12) and, (2) the observed percentage of neurons containing NFT at each year of the disease (11, our data), (Fig. 2).

The initial model, Model I, was developed in the following manner. A neuron may be modeled as being in one of 3 states: live (NFT-free), live and containing NFT, or dead. Model I assumed that neurons may die via an NFT-obligatory pathway or via a pathway in which NFT are not obligatory for cell death. In Model I we assumed all events commenced at time $t = 0$ yr, at the onset of detectable symptoms. (Later models were revised to better accommodate the fact that presymptomatic brains may contain NFT and show some degree of neuronal loss). For a first approximation, in Model I we take the initial number of neurons to be N_0 , about 13.5 million (11, 12) at time $t = 0$ yr, decaying at the rate of 500,000 per year (11) to zero at time T_{final} (the time after onset of symptoms that all neurons are dead), about 27 yr ($500,000 \times 27 = 13.5$ million), so that $N_{final} = 0$. During the intervening years, the number of neurons counted at any time (t) after the onset of symptoms was approximated by a straight line fit equal to the initial number of neurons multiplied by the quantity, 1 minus the fraction, t/T_{final} , where t is equal to time in years after the onset of symptoms and T_{final} is equal to 27 yr. This assumes that the number of neurons dying in any given year is constant, rather than proportional to the number of neurons remaining, which is consistent with the data of West (2) and Bobinski (11). This is mathematically represented by:

$$N_t = N_0 \cdot (1 - t/T_{final})$$

Where

N_t = number of CA1 neurons at any given time, t , after first report of symptoms

N_0 = number of CA1 neurons at first report of symptoms

t = any given time after first report of symptoms

T_{final} = time after first report of symptoms when all CA1 neurons have died (27 yr).

Of the total number of neurons, the fraction observed to contain NFT increases with time, as seen in Figure 2. These data are approximately fit by a fraction equal to t/T_{final} which, when multiplied by the number of observed neurons, yields the number of NFT containing neurons. This, in turn, is equal to the initial number of neurons multiplied by the quantity, 1-the fraction, t/T_{final} (27 yr), multiplied by the fraction t/T_{final} (27 yr). This is represented mathematically by:

$$NFT = (t/T_{final}) \cdot N_t = N_0 \cdot (1 - t/T_{final}) \cdot (t/T_{final})$$

This equation is plotted as "Observed NFT-Containing Neurons" in Figures 3, 4, 6, 7. Also shown in these figures are the decline of total cells, the decline of NFT-free neurons, and the number of tangle bearing neurons as a function of disease duration. All 3 of these parameters are determined by existing data and are, therefore, all fixed elements of the model. The fourth parameter, estimated survival time of neurons containing NFT, can be varied, enabling us to see which estimated survival time yields the best fit to the curves representing the observed data.

The differing assumptions underlying each of the 4 models were as follows. For Model I we assumed all events commenced at time $t = 0$ yr, at the onset of clinically detectable symptoms. We based Model I on a straight line fit to the data on the percentage of NFT vs duration of disease obtained by us and by Bobinski et al (11). In Model II we assumed NFT formation started 40 yr (6, 14) prior to the onset of symptoms. In this model, we fit 2 straight lines to the NFT percentage data, the first of which approximated the rate of formation of NFT prior to the onset of clinically detectable symptoms. Over 40 yr this line rises from zero to 8% incidence of NFT-containing live neurons at the onset of clinical disease (the average incidence of NFT-containing neurons in ours and Bobinski's nondemented control population was 8%). After the onset of symptoms we use the same rate of NFT formation as in Model I. In Model III we assumed that NFT containing neurons were dying at the same proportional rate as all neurons. We also changed the method of fitting the percentage of NFT vs duration data to an exponential curve, which smoothed the transition through yr 0, and seemed more plausible than a sharp break between 2 different rates of NFT formation. Model IV contained the same assumptions as Model III with the exception that we assumed there is only one (undefined) mechanism which kills neurons, whether they contain NFT or not. We also emphasize that changing assumptions, such as when the formation of NFT starts in relation to the onset of symptoms, changes the form of the curve that best fits the observed data.

Despite the similarity of the Bobinski data to our own (Fig. 2), we wanted to make sure that the differences in the methods used in 2 data sets did not differentially affect the model. We tested this by running Model IV separately with only the Bobinski data and again with only our data. We found no significant difference in the effect of these 2 different data sets on the

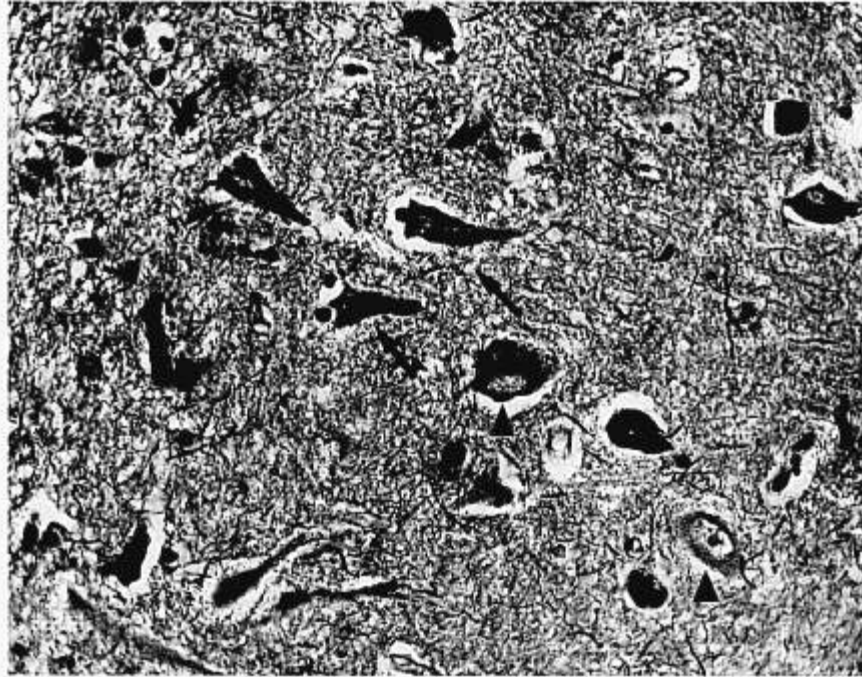


Fig. 1. Modified Bielschowski stained CA1 of an AD case to illustrate the classifications used. Long arrows illustrate neurons classified as living and containing NFT. Short arrow illustrates a ghost tangle. Arrowheads illustrate neurons classified as living and free of NFT.

model (data not shown), so the models presented here incorporate the 2 combined data sets.

RESULTS

Model I

The result obtained with Model I can be seen in Figure 3. This model fits the observed data quite closely except at very long disease duration where the model shows several hundred thousand live NFT-containing neurons left after the total number of observed neurons has reached zero. This discrepancy is due to the assumption of a latency period for NFT neurons, after which, and only after which, the neurons die. The best fit to the data was reached by assuming a 17-yr survival period for NFT containing neurons. With the assumptions made in Model I, the best fit to the observed data indicates that the maximum number of neurons containing NFT is 3.54 million, which occurs 14 yr after the onset of clinically detected disease. In the model this curve peaks at 17 yr, at which point there are 3.73 million neurons containing NFT.

The results found with Model I led us to the following preliminary conclusions: 1) A fixed 3.5% of living NFT-free neurons develop NFT each year following first report of symptoms. 2) Neurons remain alive with NFT for about 17 yr. 3) At disease duration of 27 yr, all neurons have died and one third of them contained NFT when they died.

Model II

Based on our observation that our clinically defined control population displayed an average of 8% of live neurons containing NFT, we revised Model I to account for NFT formation prior to the onset of symptoms. We postulated that tangle formation might occur 40 yr prior to the onset of clinically detectable symptoms. This is based on evidence that a small percentage of the population is observed to have NFT in their brains at ages 26–30 (6). A similarly small percentage of the population is diagnosed with AD 40 yr later at ages 65–70 (14). Likewise, at age 41–45, 40% of the brains sampled contained NFT (Stage I/II) (6) and at ages over 85 yr, about 40% of the population surveyed is diagnosed with AD (14). Previous data indicated that the rate of tangle formation during the 40 yr prior to clinical onset of disease was much slower than the rate later in the course of disease (15). We used 2 straight-line curves to fit the data on numbers of live cells with NFT. The first curve reflected a slow rate of NFT formation prior to the onset of symptoms at yr 0; the second curve a faster rate of NFT formation after the appearance of symptoms at yr 0. In addition, we needed to adjust the curve representing “total live neurons.” If tangle formation was occurring 40 yr earlier than first report of symptoms, and if NFT kill neurons, neurons must be dying in these earlier years. The average number of CA1 neurons for a control population is 13.5 million (2, 11). Since the control population

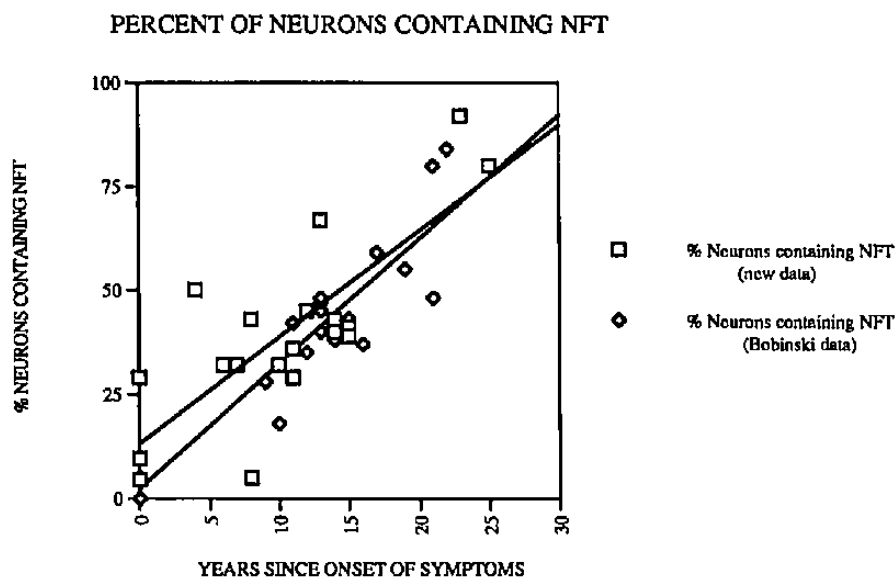


Fig. 2. Percentages of living, NFT-containing neurons as a function of disease duration. Open diamonds are the Bobinski data. Open squares are our data. We draw attention to the fact that although Bobinski et al used unbiased stereological methods and we did not, the final results are very similar. This is because we determined percentages in random fields, rather than absolute numbers, and applied these percentages to stereologically obtained data in the literature (2, 9, 10) to arrive at estimates of total numbers. The fact that this procedure yielded a close correspondence with previous data indicates that potential biases due to changes in sizes of neurons or ghost tangles did not significantly affect our data.

showed variability in the number of neurons, we let 13.5 million neurons represent yr 0 and started at yr -40 with 15.5 million neurons, which allowed a small loss of neurons prior to the development of symptoms. After the onset of symptoms, both the rate of neuron loss and the fraction of neurons developing NFT each year increased rapidly. The number of NFT containing neurons in Model II increased to a maximum of 5.80 million at a disease duration of 17 yr, after which the number, but not the percentage, of tangle bearing neurons declined. This is quite close to the observed data, which showed the maximum number of NFT-containing neurons to be 5.73 million at a disease duration of 17 yr. This revised model (Model II) can be seen in Figure 4. With Model II a curve that best fit the observed data was obtained by assuming a neuron survived with NFT for 14 yr, as compared with 17 yr in the simpler Model I. In Model II, about two thirds of the neurons died via an NFT-dependent pathway.

Model III

However, Model II still predicted a relatively large number of neurons containing NFT which were living beyond the point at which there were no longer live cells, again due to the assumption that if a neuron contains NFT, it must die via an NFT-dependent pathway. We therefore altered selected assumptions to derive Model III. For Model III, we assumed that NFT-containing neurons were dying at the same proportional rate as all live

neurons. This allowed NFT neurons to die via an undefined mechanism as well as through NFT. We assumed that all CA1 neurons were dead 30 yr after the onset of symptoms. The consequence of this change was that NFT containing neurons were not predicted to outlive the total population of neurons. Another change that was made in Model III altered the percentage of NFT containing neurons vs duration graph from a straight line to an exponential fit (Fig. 5). This exponential was used to derive the number of live neurons containing NFT each year as the disease progressed. Model III is seen in Figures 6A and B. With Model IIIA a best fit to the observed data was obtained by assuming a neuron survived with NFT for 23 yr (Fig. 6A). The observed maximum number of NFT containing neurons is 5.08 million at 21 yr. The model estimates the maximum number of NFT containing neurons at 4.60 million at 17 yr disease duration. About one fifth of the neurons died via the NFT-dependent pathway.

We also calculated Model III with the assumption that the length of time a neuron survived with NFT was approximately 15 yr, similar to Models I and II. This model graph (Model IIIB) can be seen in Figure 6B. The observed maximum number of NFT containing neurons is 5.08 million at 21 yr after onset of symptoms, while the model graph shows a peak at 15 yr of 4.09 million. About one third of the neurons died via the NFT-dependent pathway. As can be seen in the figure, this shorter survival time with NFT results in a model that no longer fits

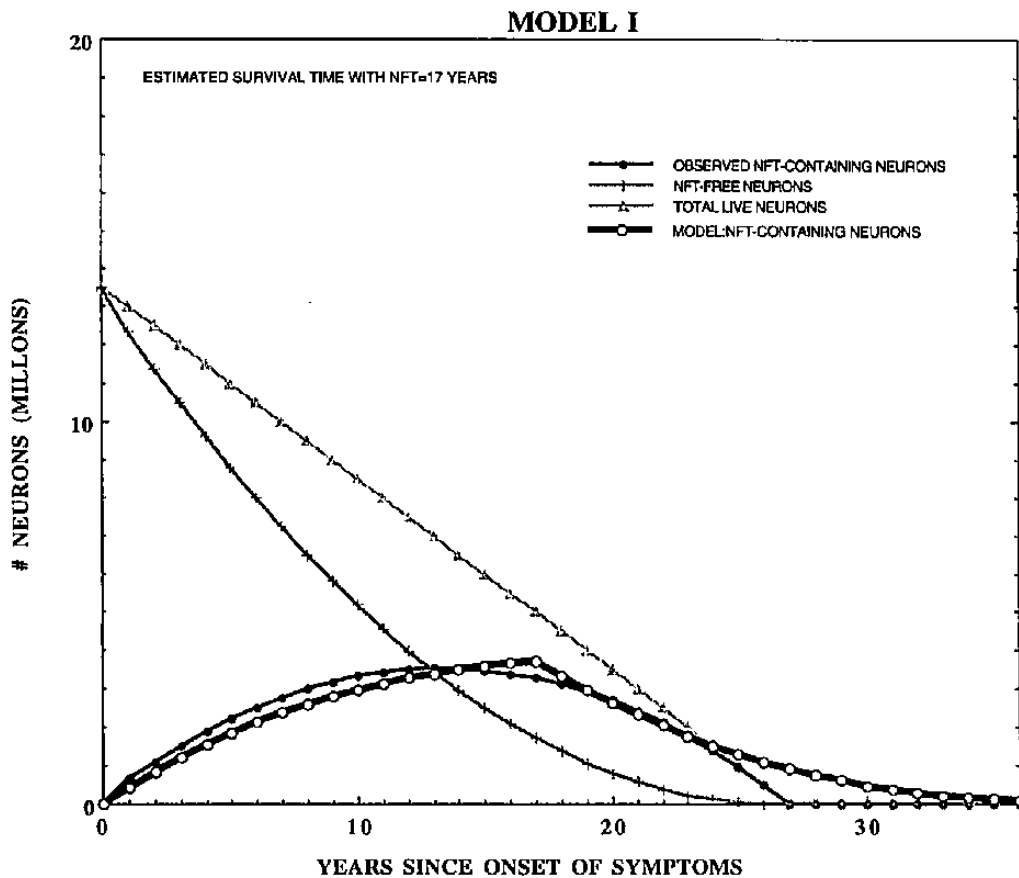


Fig. 3. Model I. This model assumes that neuron loss and NFT formation both start when symptoms of AD are first detected. Note that this model indicates significant numbers of living, NFT-containing neurons after the number of living neurons has reached zero. This is a consequence of assuming that NFT-containing neurons must die via an NFT-dependent pathway, an assumption that leads to a significant failure of the model.

the data as well. When the assumption that NFT neurons are dying at the same rate as all neurons (and not simply by an NFT-dependent mechanism) is taken into account, the period between NFT formation and neuron death as a result of NFT is increased.

Model IV

Finally, since some current data suggest NFT formation may not be obligatory for neuron death (16, 17), we derived a model that assumed neurons survived for 100 yr with NFT, which implies essentially no NFT-induced cell death at all. In this model there is only a non-NFT dependent mechanism, which kills neurons whether they contain NFT or not. As can be seen in Figure 7, Model IV more accurately fits the observed data than any of the previous 3 models (Table 2). The observed maximum number of NFT-containing live neurons is, as before, 5.08 million at 21 yr. The model shows the peak at 19 yr as 5.34 million NFT containing neurons, which is an earlier peak and more NFT-containing neurons than observed. In this model, NFT are not lethal to the neuron; the neuron will survive indefinitely unless it succumbs to a death

mechanism in which NFT formation is not obligatory. We were unable to determine if NFTs make a neuron more susceptible to the death mechanism, which is not dependent on the presence of NFT, and if so, by how much. This model assumes no preferential rate of death for NFT neurons. As seen previously, about one third of the neurons died with NFT.

DISCUSSION

The Models we have constructed derive from the proposition that when a neuronal state (such as a live neuron containing NFT) is long lasting many such neurons will be seen in sections of postmortem human brain. Conversely, if this neuronal state is short-lived, few neurons will be found to be in this state. Using recently available data to model this concept, as we have done above, leads to 2 significant but tentative conclusions: (1) A variety of assumptions lead to estimates that CA1 neurons containing NFT survive for approximately 15–25 yr on average, and (2) it is not necessary to assume that NFT cause the death of CA1 neurons in Alzheimer disease.

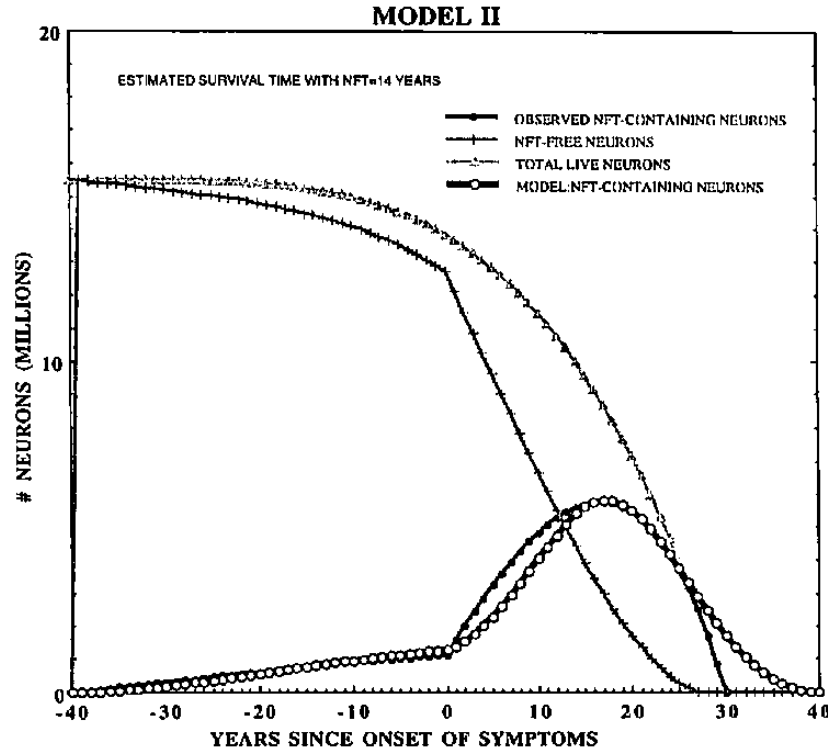


Fig. 4. Model II. Here we assume that both NFT formation and neuron loss both start 40 yr prior to when symptoms of AD are first detected. Both of these are assumed to progress at a slow linear rate (see text) prior to appearance of symptoms and then accelerate after symptoms appear. This model also indicates significant numbers of living, NFT-containing neurons after the number of living neurons has reached zero.

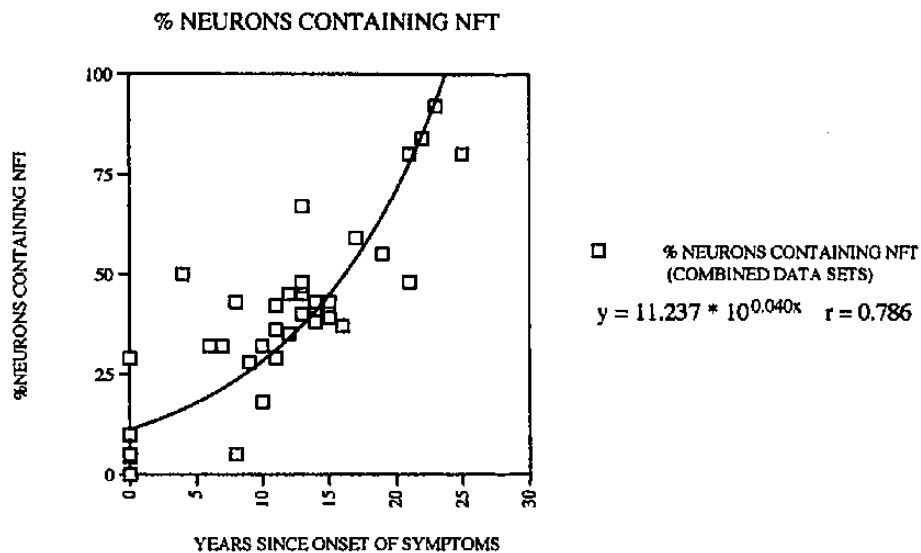


Fig. 5. An exponential fit to the observed data describing percentage of neurons that contain NFT as a function of disease duration. Bobinski data and our data combined.

Since our data, as well as the data of Bobinski et al (11) were based on pyramidal neurons in the CA1 zone of the hippocampus, the conclusions of both these papers must be limited to this cell population. The extent to which the above conclusions may be generalized to other

cell types in other locations remains an open question that has interesting implications for the role of NFT in the biology of the cell. We would point out, however, that CA1 of hippocampus has been particularly propitious for studies of this nature due, in large part, both to the

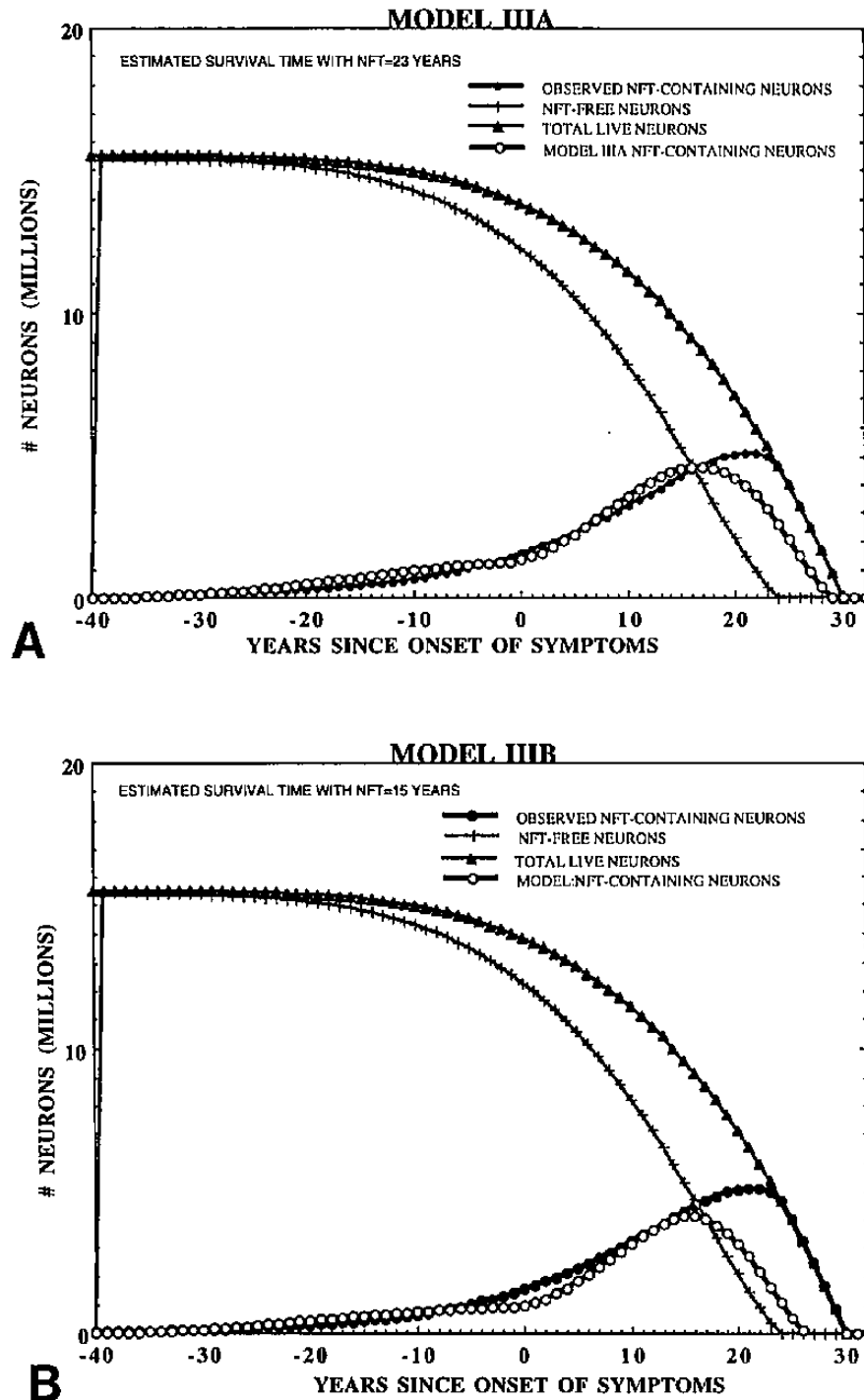


Fig. 6. Model III. Two major assumptions were altered to produce Model III. It is now assumed that neurons containing NFT die at a rate that is proportional to the number of live neurons. This removes the requirement that all NFT containing neurons must die through an NFT-dependent pathway, and allows other, undefined, mechanisms of neuron death to play a role. It is also assumed that an exponential, rather than 2 straight lines, provided a better fit to the data expressing the percentage of neurons containing NFT as a function of disease duration. Models IIIA and IIIB illustrate the effect of assuming different survival times for a neuron containing NFT—23 yr for IIIA and 15 yr for IIIB. Both of these models arrive at predictions which depart significantly from the observed data at longer disease duration.

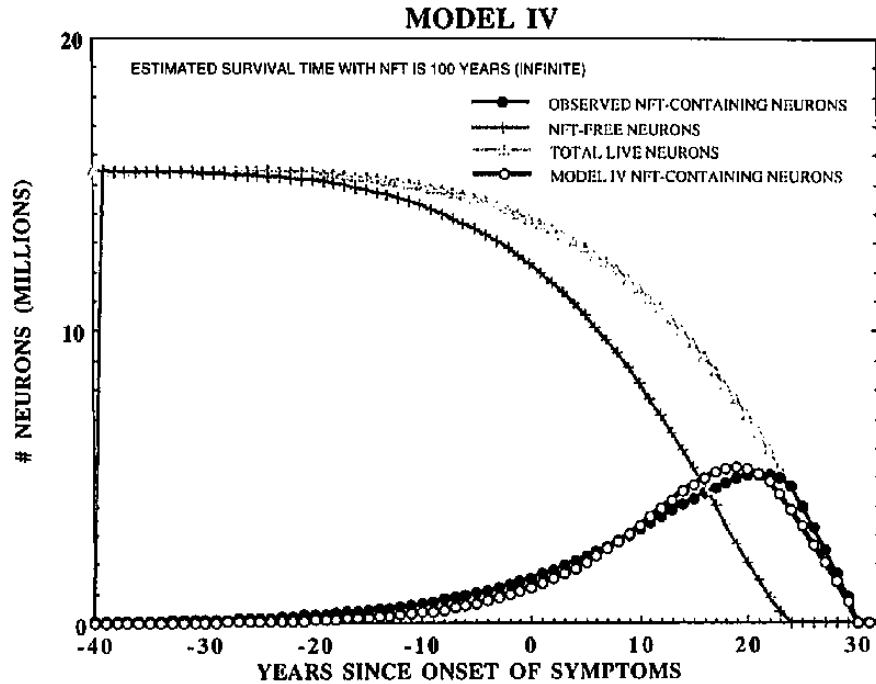


Fig. 7. Model IV. In this model all assumptions are similar to those in Model III with the exception that we now assume that NFT are not lethal to neurons. The fit to the observed data is excellent when we model an average survival time of neurons with NFT as being 100 yr, which in effect, indicates an infinite survival time.

TABLE 2
Parameters of Models

	Model I	Model II	Model IIIA	Model IIIB	Model IV
Maximum # of NFT containing neurons observed (millions)	3.54	5.73	5.08	5.08	5.08
Maximum # of NFT containing neurons predicted by model (millions)	3.73	5.80	4.60	4.09	5.34
Years duration at maximum numbers of NFT neurons observed (since onset of symptoms)	14	17	21	21	21
Years duration at maximum number of NFT neurons predicted by model (since onset of symptoms)	17	17	17	15	19
Neuron survival time with NFT (yr)	17	14	23	15	100
Percentage of neurons that die via NFT mechanism	28%	66%	19%	38%	0

formation of NFT in significant numbers and to the relative ease of defining boundaries and cell types. Unfortunately, the extension of unbiased stereology to most neocortical areas has proved to be considerably more challenging due to difficulties in defining boundaries, and the relative vastness of most of these regions (18). However, the entorhinal cortex offers one potentially promising neocortical region for further study (see ref. 16 for example).

A recent publication (19) estimates the duration of neurofibrillary change in CA1 of hippocampus as 3.4 yr, with neurofibrillary change defined as time from first appearance of neurofibrillary pathology to time when a ghost tangle appears. Since our 4 models and their analysis are based on greatly overlapping, though not identical data

sets, we suggest that the difference between their estimate of 3.4 yr and our estimate of 15–25 yr is based on differences in analytical approaches used and assumptions made. The conclusions of Bobinski et al (19) are based on using a regression analysis to estimate the time at which the onset of NFT occurred in all intact neurons, as well as the time in which all neurons with NFT became ghost tangles (i.e. died). The Bobinski et al analysis assumes that all neurons develop NFT and, consequently, that all neurons die through a mechanism that requires the formation of NFT. On the other hand, we found that our models did not fit the data if we required that all neurons develop NFT before they die. Further, a conclusion that all neurons must develop NFT before they die is inconsistent with the data of Gomez-Isla et al referred to below.

Our conclusion as to the length of time a neuron survives with NFT is consistent with the biochemical data of Kenessey et al (20). They determined the amount of D-aspartate to be 2.82% in normal tau and about 4.9% in PHF tau. Since the rate of racemization of aspartic acid to D-aspartate in a number of proteins is about 0.1% per yr at 37°C in vivo (21), the authors conclude "it would then take several decades for a newly generated tau to reach the state of D-aspartate detected in PHF-tau." More precisely, the approximately 2% difference in D-aspartate between N-tau and PHF-tau yields an estimate of about 20 yr for PHF-tau to reach the degree of racemization determined by Kenessey et al.

Our conclusion that it is not necessary to assume that NFT cause the death of neurons in Alzheimer disease is also consistent with recent findings from other laboratories. For example, Gomez-Isla et al (16, 17) report that although the amount of neuronal death and the percentage of tangle bearing neurons increase in parallel over the duration of the disease, estimated neuron death exceeds (by 7- to 10-fold) the numbers of NFT in the superior temporal sulcus and the entorhinal cortex of AD brains (16, 17). These studies of Gomez-Isla et al do not require that NFT formation be obligatory for cell death, only that NFT be related in some way to cell death pathways. The concept of uncoupling neuronal cell death from NFT is further supported by the recent work of Grignon et al (22) and Sheng et al (23), who show that TUNEL positivity (which is often equated with DNA damage) is not necessarily tangle dependent.

The probability that an NFT-bearing neuron may survive for as long as 20 yr does not mean that it is functioning normally during that time. In fact, the evidence suggests there are major changes in gene expression in such neurons. These changes in gene expression reduce expression of molecules related to synaptic function, energy metabolism and neuronal plasticity (9, 10, 24). At the same time, there is also increased expression of molecules related to stress responses, cell cycle, and apoptosis, etc. (25, 26, 27, 28). Thus, although NFT-bearing neurons continue to survive, the presence of NFT is associated with a number of alterations in the profile of gene expression of individual neurons that represents an alteration of the normal functioning of the neuron.

If NFT formation is not an obligatory stage on the way to cell death as suggested by Model IV, as well as by data of others, then how may NFT be related to the pathophysiological cascade of AD? We suggest that some event(s) initiate a signaling cascade that leads to both neuron death and the formation of NFT. For example, it has been shown that A β is toxic to neurons in culture (29, 30, 31, 32), and also that it can induce expression of molecules and genes associated with the cell cycle and apoptosis such as cyclin B, cdk-4, p16, c-jun, c-fos (23, 26, 27) and MAP kinase (33, 34, 35, 36). MAP kinase

has been shown to activate several kinases that are associated with both the cell cycle and with tau phosphorylation, and it has been suggested that MAP kinase may play an intermediary role between A β and the formation of NFT (35). In addition, A β has been shown to induce tau phosphorylation in vitro as well as immunoreactivity to antibodies often used to reveal tau pathology in AD (36, 37, 38). Thus, A β , or some other initiating event may lead to a reactivation of expression profiles normally associated with cell division very early in the life history of a neuron. However, since the mature neuron is now committed to being postmitotic, this expression profile may lead to neuron death by a pathway which also produces NFT as an offshoot of the signal cascade that leads to the death of neurons.

The analytical approach employed here is, of course, not limited to neuronal survival with NFT, but may be applied to any definable state of any cell in any tissue. We are currently in process of applying this approach to estimate the time that neurons spend in other states of interest in Alzheimer disease.

REFERENCES

1. The National Institute on Aging and Reagan Institute Working Group on diagnostic criteria for the neuropathological assessment of Alzheimer's disease. Consensus recommendations for the post-mortem diagnosis of Alzheimer's disease. *Neurobiol Aging* 1997; 18:S1-S2
2. West MJ, Coleman PD, Flood DG, Troncosco JC. Differences in the pattern of hippocampal neuronal loss in normal aging and Alzheimer's disease. *Lancet* 1994;344:769-72
3. Morris JC, McKeel DW, Storandt M, et al. Very mild Alzheimer's disease: Informant based clinical, psychometric, and pathological distinction from normal aging. *Neurology* 1991;41:469-78
4. Crystal H, Dickson D, Fuld P, et al. Clinico-pathologic studies in dementia: Nondemented subjects with pathologically confirmed Alzheimer's disease. *Neurology* 1988;38:1682-87
5. Arriagada PV, Marzloff K, Hyman BT. Distribution of Alzheimer-type pathologic changes in nondemented elderly individuals matches the pattern in Alzheimer's disease. *Neurology* 1992b;42:1681-88
6. Braak H, Braak E. Frequency of stages of Alzheimer-related lesions in different age categories. *Neurobiol Aging* 1997;18:351-57
7. Griffin WS, Ling C, White CL, Morrison-Bogorad M. Polyadenylated messenger RNA in paired helical filament-immunoreactive neurons in Alzheimer disease. *Alzheimer Dis Assoc Disord*. 1990; 4:69-78
8. Doebler JA, Markesbery WR, Anthony A, Davies P, Scheff SW, Rhoads RE. Neuronal RNA in relation to Alz-50 immunoreactivity in Alzheimer's disease. *Ann Neurol*. 1988;23:20-24
9. Callahan LM, Selski DJ, Martzen MR, Cheetham JE, Coleman PD. Preliminary evidence: Decreased GAP-43 message in tangle-bearing neurons relative to adjacent tangle-free neurons in Alzheimer's disease parahippocampal gyrus. *Neurobiol Aging* 1994;15:381-86
10. Callahan LM, Coleman PD. Neurons bearing neurofibrillary tangles are responsible for selected synaptic deficits in Alzheimer's disease. *Neurobiol Aging* 1995;16:311-14
11. Bobinski M, Wegiel J, Tarnawski M, et al. Relationships between regional neuronal loss and neurofibrillary changes in the hippocampal formation and duration and severity of Alzheimer disease. *J Neuropath Exp Neurol* 1997;56:414-20

12. West MJ. Regionally specific loss of neurons in the aging human hippocampus. *Neurobiol Aging* 1993;14:287-93
13. Yamamoto T, Hirano A. A comparative study of Modified Bielschowsky, Bodian, and Thioflavin S stains on Alzheimer's neurofibrillary tangles. *J Neuropathol Appl Neurobiol* 1986; 12: No.3-9
14. Breteler MMB, Claus JJ, van Duijn CM, Launer LJ, Hofman A. Epidemiology of Alzheimer's disease. *Epidemiol Rev* 1992;14:59-82
15. Ohm TG, Muller H, Braak H, Bohl J. Close-meshed prevalence rates of different stages as a tool to uncover the rate of Alzheimer's disease-related neurofibrillary changes. *Neurosci* 1995;64:209-17
16. Gomez-Isia T, Price JL, McKeel DW, Morris JC, Growdon JH, Hyman BT. Profound loss of layer II entorhinal cortex neurons occurs in very mild Alzheimer's disease. *J Neurosci* 1996;16:4491-5000
17. Gomez-Isla T, Hollister R, West H, et al. Neuronal loss correlates with but exceeds neurofibrillary tangles in Alzheimer's disease. *Ann Neurol* 1997;41:17-24
18. Regeur L, Jensen GB, Pakkenberg H, Evans SM, Pakkenberg B. No global neocortical nerve-cell loss in brains from patients with senile dementia of the Alzheimer's type. *Neurobiology of Aging* 1994;15:347-52
19. Bobinski M, Wegiel J, Tarnawski M, et al. Duration of neurofibrillary changes in the hippocampal pyramidal neurons. *Brain Res* (In Press)
20. Kenessey A, Yen SH, Liu WK, Yang XR, Dunlop DS. Detection of D-aspartate in tau proteins associated with Alzheimer paired helical filaments. *Br Res* 1995;675:183-89
21. Bada JL. Racemization of amino acids. In: G.C. Barrett, ed. *Chemistry and Biochemistry of the Amino Acids*. New York: Chapman and Hall, 1985:399-414
22. Grignon Y, Duyckaerts C, Bannicib M, Hauw JJ. Cytoarchitectonic alterations in the supramarginal gyrus of late onset Alzheimer's disease. *Acta Neuropathol* 1998;95:395-406
23. Sheng JG, Mrak RE, Griffin WST. Progressive neuronal DNA damage associated with neurofibrillary tangle formation in Alzheimer disease. *J Neuropathol Exp Neurol* 1998;57:323-28
24. Hatanpaa K, Brady DR, Stoll J, Rapoport SI, Chandrasekaran K. Neuronal activity and early neurofibrillary tangles in Alzheimer's disease. *Ann Neurol* 1996;40:411-20
25. Chow N, Cox C, Callahan LM, Weimer JM, Guo L, Coleman PD. Expression profiles of multiple genes in single neurons of Alzheimer's disease. *Proc Natl Acad Sci USA* (In Press)
26. McShea A, Harris PLR, Webster KR, Wahl AF, Smith MA. Abnormal expression of the cell cycle regulators P16 and CDK4 in Alzheimer's disease. *Amer J Pathol* 1997;150:1933-39
27. Nagy Z, Esiri MM, Cato AM, Smith AD. Cell cycle markers in the hippocampus in Alzheimer's disease. *Acta Neuropathol* 1997;94:6-15
28. Liu WK, Williams RT, Hall FL, Dickson DW, Yen SH. Detection of a CDC2-related kinase associated with Alzheimer's paired helical filament. *Amer J Pathol* 1995;146:228-38
29. Estus S, Tucker HM, vanRooyen C, et al. Aggregated amyloid-beta protein induces cortical neuronal apoptosis and concomitant apoptotic pattern of gene induction. *J Neurosci* 1997;17:7736-45
30. Li YP, Bushnell AF, Lee CM, Perlmutter LS, Wong SK. Beta-amyloid induces apoptosis in human-derived neurotypic SH-SY5Y cells. *Brain Res* 1996;738:196-204
31. Forloni G, Chiesa R, Smiroldo S, et al. Apoptosis mediated neurotoxicity induced by chronic application of beta amyloid fragment 25-35. *Neuroreport* 1993;4:523-26
32. Gschwind M, Huber G. Apoptotic cell death induced by beta-amyloid (1-42) peptide is cell type dependent. *J Neurochem* 1995;65:292-300
33. Anderson AJ, Pike CJ, Cotman CW. Differential induction of immediate early gene proteins in cultured neurons by beta-amyloid (A-beta): association of c-jun with A-beta induced apoptosis. *J Neurochem* 1995;1487-98
34. Greenberg SM, Koo EH, Selkoe DJ, Qiu WQ, Kosik KS. Secreted beta-amyloid precursor protein stimulates mitogen-activated protein kinase and enhances tau phosphorylation. *Proc Natl Acad Sci USA* 1994;91:7104-8
35. Greenberg SM, Qiu WQ, Selkoe DJ, Benitezhak A, Kosik KS. Amino-terminal region of the beta-amyloid precursor protein activates mitogen-activated protein kinase. *Neurosci Lett* 1995a;198:52-56
36. Greenberg SM, Kosik KS. Secreted beta-APP stimulates MAP kinase and phosphorylation of tau in neurons. *Neurobiol Aging* 1995b;16:403-7
37. Ferreira A, Lu Q, Orecchio L, Kosik KS. Selective phosphorylation of adult tau isoforms in mature hippocampal neurons exposed to fibrillar A beta. *Mol Cell Neurosci* 1997;9:220-34
38. Bucigilio J, Lorenzo A, Yeh J, Yankner B. Beta-amyloid fibrils induce tau phosphorylation and loss of microtubule binding. *Neuron* 1995;14:879-88

Received July 17, 1998

Revision received November 4, 1998

Accepted November 6, 1998